GaAs-$Al_xGa_{1-x}As$ double-barrier heterostructure phonon laser: A full quantum treatment

I. Camps,[1] S. S. Makler,[1,2] H. M. Pastawski,[3] and L. E. F. Foa Torres[3]
[1]*Instituto de Física, Universidade Federal Fluminense, Niteróí, Rio de Janeiro, Brazil*
[2]*Instituto de Física, Universidade do Estado de Rio de Janeiro, Rio de Janeiro, Brazil*
[3]*FaMAF, Universidad Nacional de Córdoba, 5000 Córdoba, Argentina*

(Received 21 December 2000; revised manuscript received 4 April 2001; published 10 September 2001)

The aim of this work is to describe the behavior of a device capable to generate high-frequency (~THz) acoustic phonons. This device consists in a GaAs-$Al_xGa_{1-x}As$ double-barrier heterostructure that, when an external bias is applied, produces a high rate of longitudinal optical (LO) phonons. These LO phonons are confined and they decay by stimulated emission of a pair of secondary longitudinal optical $(\widetilde{\mathrm{LO}})$ and transversal acoustic phonons. The last ones form an intense beam of coherent acoustic phonons. To study this effect, we start from a tight-binding Hamiltonian that takes into account the electron-phonon and phonon-phonon interactions. We calculate the electronic current through the double barrier and obtain a set of five coupled kinetic equations that describes the electron and phonon populations. The results obtained here confirm the behavior of the terahertz phonon laser, estimated by rougher treatments [S.S. Makler *et al.*, J. Phys.: Condens. Matter **10**, 5905 (1998).]

DOI: 10.1103/PhysRevB.64.125311 PACS number(s): 73.23.−b, 73.40.Gk, 63.20.Kr

I. INTRODUCTION

Since the pioneering experiments of Chang, Esaki and Tsu,[2] the tunneling processes in semiconductor heterostructures have attracted great interest. This has been increasing with the development of modern deposition techniques such as metal-organic chemical-vapor deposition and molecular beam epitaxy that can provide artificial nanostructures. Such structures, coupled to electrical leads, can display many unusual behaviors.

Most of works have focused on electron transport phenomena through heterostructure devices. The double-barrier heterostructure (DBH) permits the creation of several kinds of electronic devices such as semiconductor laser diodes, ultrahigh-frequency oscillators, and many others.[3]

One of the most important problems in the study of resonant tunneling in DBH is the electron-phonon (e-ph) interaction. After the works of Goldman, Tsui, and Cunningham,[4,5] the importance of electron-phonon interaction on the electronic properties of these structures was realized. However, little importance has been given to the study of the phonons generated in this process, the way they propagate, their decay processes, etc.

Our purpose is to study the phonon generation in a DBH under the effect of an external applied bias. Our device consists in a DBH made of GaAs-$Al_xGa_{1-x}As$. It was designed in such a way that the difference $\Delta\varepsilon$ between the first excited level ε_1 and the ground state ε_0 in the well is of the order of the longitudinal optical (LO) phonon energy $\hbar\omega_1$, for a small applied bias V. Here, ω_1 is the Γ-point LO phonon frequency. The Fermi level ε_F^L in the emitter is such that the excited level is above it. With a further increase in V, the levels in the well are lowered relative to ε_F^L. When the ground state comes under the bottom of the conduction band, the current is almost suppressed until the level ε_1 reaches ε_F^L. To continue increasing V, the current begins to flow through the excited level, but since $\Delta\varepsilon$ remains less than $\hbar\omega_1$, the phonon emission is inhibited. For a given bias V the resonant condition $\Delta\varepsilon \approx \hbar\omega_1$ is achieved and the electrons begin to decay to the ground state by emitting primary LO phonons. The potential profile and the level positions at this resonant condition are shown in Fig. 1.

For an Al concentration greater than 0.25 (Ref. 6) or 0.3 (Ref. 7), these phonons are confined to the well (they can be also absorbed by exciting electrons from ε_0 to ε_1).

The process described above, acts in parallel with the decay of primary LO phonons due to anharmonicity. One product of this decay is a secondary longitudinal optical phonon $(\widetilde{\mathrm{LO}})$, the other is a transversal acoustic (TA) phonon.[8,9] The $\widetilde{\mathrm{LO}}$-TA pair is produced by stimulated emission. Therefore these TA phonons, for a bias greater than the operation threshold, are coherent and form a beam that we call saser by analogy with a laser. The coherence of the device presented here was studied previously[10] by developing a formalism similar to that employed usually to study the coherence in lasers[11,12] that take into account the competition among the several emitted modes.

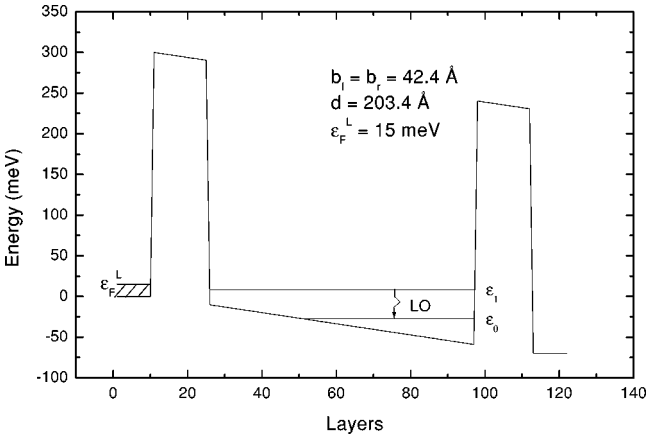

FIG. 1. Potential profile and energy levels at the resonant condition. $b_l(b_r)$ and d are the barriers and well width, respectively.

In the early 1960's,[13] generation of coherent phonons was discussed theoretically and observed experimentally.[14,15] Several experiments and applications were suggested.[16] These phonons can be generated by intense pulses of laser.[17–21] More details were described in the review of Kurz and co-workers.[22] In a recent review, Merlin[23] discusses the generation of pulses of coherent terahertz optical phonons by intense femtosecond-pulsed lasers.

Coherent acoustic phonons can be also obtained with a wavelength given by the period of the superlattice where phonons are optically generated (i.e., 500 Å).[24] In our case, the system generates coherent sound by electronic means with much shorter wavelength. The generation of high-frequency monochromatic acoustic waves by laser-induced thermomodulation was reported by Damen *et al.*[25] The phonon frequency ranged from 2 to 4 GHz comparing with 2 THz for our device.

Generation of phonons by stimulated emission was theoretically considered[26] and observed experimentally. Bron and Grill[27] reported the direct observation of the stimulated emission of 24.7 cm^{-1} phonons in a three-level system of V^{4+} ions in Al_2O_3. Prieur *et al.*[28,29] studied the phonon emission in a two-level system of a glass. These phonons had a wide frequency distribution around $\omega = 0.34$ GHz. Zavtrak and collaborators[30–35] proposed a device consisting in a dielectric liquid with small particles or gas bubbles working in a way similar to a free-electron laser. That device could produce coherent acoustic phonons by stimulated emission at a frequency $\omega \approx 2$ KHz. Stimulated emission of phonons in an acoustic cavity was obtained experimentally by Fokker *et al.*[36,37] They used the metastable Zeeman-split doublet in ruby. These phonons have frequencies of about 60 MHz.

At present, several kinds of amplified coherent beams of bosons are produced by stimulated emission. Besides the traditional visible or near-infrared photons (lasers) and microwave photons (masers), other coherent photon beams are produced. High-energy lasing processes like x-ray lasers (called also xasers)[38,39] and gamma-ray lasers (GRASERS)[40] were studied.

A very exciting field has recently opened with the development of atoms lasers.[41–44] Several applications of these novel devices, such as high-precision gravimetry, are proposed. Strongly related to this is the study of vibrational amplification by stimulated emission of radiation (vaser).[45]

Kleppner[46] voices concern against that complicated jargon of acronyms and proposes to simplify to atom laser, x-ray laser, etc.

In summary, a great effort has been made to produce terahertz phonons using other mechanisms different than stimulated emission. On the other side, acoustic phonons have been produced by stimulated emission but at frequencies lower than 2 THz. The DBH resonator proposed here could produce a continuous beam of terahertz coherent phonons. The ultrashort wavelength of these phonons permits potential applications.

Acoustic imaging is a very well-known procedure, mainly in medicine, where the fact that different water contents on several tissues produce different attenuations for a signal of about 4 MHz is exploited. Today commercial equipments are available that can produce three-dimensional images of very high resolution.

Equipments for acoustic microscopy are less known but they are also commercially available. The most used technique is scanning acoustic microscopy[47] that can attain resolutions higher than 0.4 μm, taken with phonons of 2 GHz.

Besides the scanning acoustic microscopy, several techniques have been presented in a recent review:[48] photoacoustic microscopy, scanning electron acoustic microscopy, and scanning laser acoustic microscopy. The theory of acoustic imaging was also reviewed, schematic diagrams of the different microscopes are presented and several industrial applications are discussed in Ref. 48.

The equipments mentioned above work at up to 10 GHz, three orders of magnitude lower than the frequency of the phonon beam considered in the present paper. Therefore they have a limited theoretical resolution given by its wavelength that is one thousand times greater than that generated by a DBH device.

To make the acoustic nanoscopy possible, it is necessary to have a coherent beam of ultra-short-wavelength phonons. To obtain images of a small structure, one would need waves shorter than the size of the details of the system.

Maris[49] describes the process of acoustic nanoscopy by means of echoes of ultrashort phonon pulses optically generated. They are detected by measuring the variation of optical reflectivity due to the scattered phonon pulses. They work with coherent phonons of about 2 THz like those produced by our device, but they were not produced by a phonon laser.

Evidently, a laser is not necessary to produce optical images. Nevertheless, lasers are a very useful tool for imaging and up today they are indispensable to make holograms. On the other hand, many optical experiments that can be performed with incoherent light are done more easily and more precisely with the aid of a laser. Therefore many experiments that are performed today with incoherent phonons could be done better with the aid of a phonon laser.

The phonon laser described in this paper has a wavelength smaller than 25 Å (that is about 20 times less than for the device described in Ref. 24). Therefore it is possible to use it to see structures of about 50 nm. A coherent source of x rays of about 20 nm begins to be available now.[50,51] Even if it will be possible to make images of structures at the submicron scale by using x rays of a wavelength of about 25 Å , they would have energies of about 0.5 KeV, what could affect the system to be studied.

The device presented here could be used to get a hologram at nanoscale. To do this, it is possible to build in a GaAs an acoustic analogous of a Michelson interferometer. It consists of a thin barrier of $Al_xGa_{1-x}As$ designed as a semimirror, placed at 45° to split the beam and to force it to pass one half through the part of the sample we are interested in and the other across a very pure reference GaAs. After that, we can use mirrors (made of thick $Al_xGa_{1-x}As$ barriers) to superpose them and record the interference pattern with a detector. This pattern could be processed in a computer to get a hologram of the sample showing the three-dimensional shape of the nanostructure. In a previous paper[1] we de-

scribed, as an alternative, the acoustic version of a Sagnac interferometer.

Because of the high sensitivity to all types of lattice defects, the phonon beam could be used to give information about the inner lattice structure,[52,49] and form part of a phonon imaging setup as a source.[53]

We will show that the amplitude of the phonon beam is with a great precision directly proportional to the incoming current. Therefore the saser amplitude could be modulated by modulating the amplitude of the current. This will permit the use of the phonon laser as an information carrier between circuit components at very short distances. These ''phonoelectronic'' devices could work at smaller distances and lower energies than optoelectronic devices.

If we achieve to make a ''phonoresist,'' i.e., a material with a soft mode close to the frequency of our phonon laser, the saser could be used for nanolithography. Due to the short wavelength and low energy of the phonon beam, ''phonolithography'' would be a better option than the methods currently in use.

The potencial applications of the device described above could be inhibited by several shortcomings. The lifetime of TA phonons could be limited at finite temperatures. Besides, the inelastic scattering of the emitted phonons could be also a limitation. However, images with terahertz phonons were obtained (with coherent phonons generated in alternative forms),[52,49] showing that these shortcomings could be overcame.

The rest of this paper is organized as follows. The Hamiltonian that describes our system is presented in Sec. II. The solutions of the Hamiltonian are obtained is Sec. III. In Sec. IV, we show the procedure used to obtain the kinetic equations. We devote Sec. V to present our results and conclusions.

II. THE HAMILTONIAN

To describe our system, we considered a Hamiltonian composed of a single particle part and one representing the interactions. The single particle part can be written as

$$\mathcal{H}_o=\mathcal{H}_e+\mathcal{H}_1+\mathcal{H}_2+\mathcal{H}_3, \tag{1}$$

where $\mathcal{H}_e$ describes the electrons, and $\mathcal{H}_1$, $\mathcal{H}_2$, $\mathcal{H}_3$ the LO, $\widetilde{\mathrm{LO}}$, and TA phonons, respectively.

Assuming the grown direction as the z axis, the Hamiltonians $\mathcal{H}_1$, $\mathcal{H}_2$, $\mathcal{H}_3$ for the phonons can be written

$$\mathcal{H}_1=\sum_{\mathbf{q}_1}\hbar\omega_1 b^\dagger_{1_{\mathbf{q}_1}} b_{1_{\mathbf{q}_1}}, \tag{2}$$

$$\mathcal{H}_2=\sum_{\mathbf{q}_2}(\hbar\omega_2-i\hbar\kappa_2) b^\dagger_{2_{\mathbf{q}_2}} b_{2_{\mathbf{q}_2}}, \tag{3}$$

$$\mathcal{H}_3=\sum_{\mathbf{q}_3}(\hbar\omega_3-i\hbar\kappa_3) b^\dagger_{3_{\mathbf{q}_3}} b_{3_{\mathbf{q}_3}}, \tag{4}$$

where $\hbar\omega_1$, $\hbar\omega_2$, $\hbar\omega_3$ are the energies for LO, $\widetilde{\mathrm{LO}}$, and TA phonons, respectively, and $b^\dagger_{i_{\mathbf{q}_i}}$ ($b_{i_{\mathbf{q}_i}}$) are the creation (annihilation) operators for phonons with momentum $\mathbf{q}_i$ perpendicular to the z direction. Two imaginary terms ($i\hbar\kappa_2, i\hbar\kappa_3$) were introduced to take into account the decay by anharmonicity of the $\widetilde{\mathrm{LO}}$ phonons and the escape of the TA phonons, respectively.

To describe the electrons, we use a tight-binding approach with hoppings v between nearest neighbors. Writing the Hamiltonian in a Wannier basis, in terms of the electronic creation (annihilation) operators $c^\dagger_{\mathbf{r}}(c_{\mathbf{r}})$ at site $\mathbf{r}$, we get

$$\mathcal{H}_e=\sum_{\mathbf{r}}\varepsilon_{\mathbf{r}}c^\dagger_{\mathbf{r}}c_{\mathbf{r}}+v\sum_{\langle\mathbf{r},\mathbf{r}'\rangle}(c^\dagger_{\mathbf{r}}c_{\mathbf{r}'}+c^\dagger_{\mathbf{r}'}c_{\mathbf{r}}), \tag{5}$$

where $\mathbf{r}\equiv(l,m,j)$ with l, m, $j=-\infty,\ldots,\infty$. As the system has no magnetic behavior the subscript σ (for spin) is left implicit.

Our system has translational symmetry in the perpendicular directions (xy). Therefore the Hamiltonian can be uncoupled by expanding the operators $c_{\mathbf{r}}$ in plane waves in these directions

$$c_{\mathbf{r}}=\sum_{\mathbf{k}} c_{j\mathbf{k}}e^{i\mathbf{k}\cdot\mathbf{x}_{lm}}. \tag{6}$$

We can treat the system as a sum over one-dimensional Hamiltonians for each wave vector $\mathbf{k}$ perpendicular to the current z direction

$$\mathcal{H}_e=\sum_{\mathbf{k}}\left\{\sum_j\tilde{\varepsilon}_{j\mathbf{k}}c^\dagger_{j\mathbf{k}}c_{j\mathbf{k}}+v\sum_{\langle jj'\rangle}(c^\dagger_{j\mathbf{k}}c_{j'\mathbf{k}}+c^\dagger_{j'\mathbf{k}}c_{j\mathbf{k}})\right\}, \tag{7}$$

where $\tilde{\varepsilon}_{j\mathbf{k}}=\varepsilon_{j\mathbf{k}}-4v$. The energies $\tilde{\varepsilon}_{j\mathbf{k}}$ are measured from the bottom of the conduction band of the emitter and $\varepsilon_{j\mathbf{k}}=\varepsilon_j+\varepsilon_{\mathbf{k}}$. The energies ε_j are chosen to describe the energy profile of the DBH. For the sake of simplicity, we will leave implicit the dependence on $\mathbf{k}$.

For the z direction, we separate the space in three regions: the dispersion region and two semi-infinite one-dimensional chains. On the left we will have planes with energy $\varepsilon_j=0$ for $j\leqslant 0$ and to the right $\varepsilon_j=V$ for $j\geqslant L+1$, L is the length of the DBH. The corresponding eigenstates of these two regions are planes waves. If we disconnect the DBH from the left and right chains we get for the dispersion region the profile of an infinite (even not rectangular) well as it is shown in Fig. 2.

For the dispersion region, we diagonalize a three-diagonal matrix of order L corresponding to the profile showed above getting the eigenvalues ε_m and the eigenvectors $|m\rangle$ of equation

$$\mathcal{H}'_{ez}|m\rangle=\varepsilon_m|m\rangle. \tag{8}$$

Here, $\mathcal{H}'_{ez}$ is the part of $\mathcal{H}_{ez}$ that goes from the beginning of the left barrier to the end of the right one. Written in the basis of planes this is,

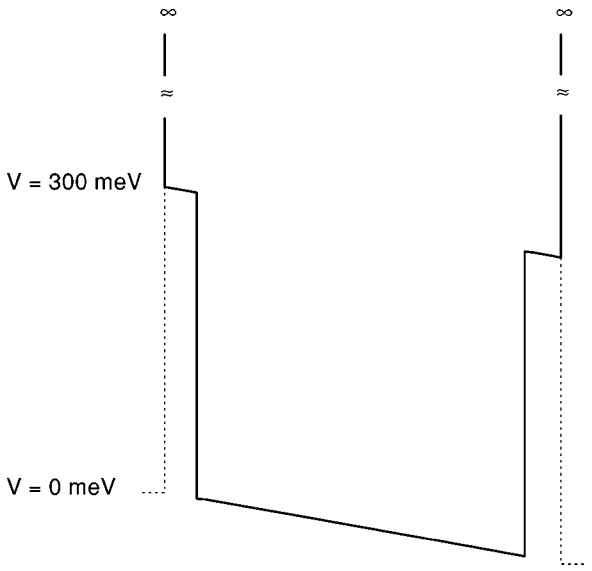

FIG. 2. The profile for the scattering region.

$$\mathcal{H}'_{ez}=\begin{pmatrix} \tilde{\varepsilon}_1 & v & 0 & & & \\ v & \tilde{\varepsilon}_2 & v & & & \\ 0 & v & \tilde{\varepsilon}_3 & \ddots & & \\ & & \ddots & \ddots & & \\ & & & & v & \\ & & & v & \tilde{\varepsilon}_L \end{pmatrix}, \tag{9}$$

where $\tilde{\varepsilon}_j=\varepsilon_j-2v$.

After the diagonalization we get L discrete levels. We label these levels through the index m as $m=0, 1', 2' \ldots$. For the right chain we rename the planes, from $L+1$, $L+2$, ... to 1, 2, ...; and for the left one, from 0, -1, -2, ..., $-\infty$ to $\overline{1}$, $\overline{2}$, ..., $\overline{\infty}$. Therefore we get a new picture where we have two semi-infinite chains, the first one corresponding to the planes $j=\overline{\infty}, \ldots, \overline{1}$ and the other one corresponding to $j=1, \ldots, \infty$. Among the L levels obtained from the diagonalization of the matrix (9), only the two states with lowest energies will participate significantly in the electronic transport. The others are far over the Fermi level and their effects will be considered later.

To connect the DBH with the left and right chains we compute the matrix elements

$$v_{jm}=\langle j|\mathcal{H}_{ez}|m\rangle. \tag{10}$$

The electronic Hamiltonian is

$$\mathcal{H}_e=\sum_j \varepsilon_j c_j^\dagger c_j+\sum_m \varepsilon_m c_m^\dagger c_m+\sum_{j\neq 1,m} v(c_j^\dagger c_{j+1}+c_{j+1}^\dagger c_j)$$
$$+\sum_m \{v_{\overline{1}m}(c_{\overline{1}}^\dagger c_m+c_m^\dagger c_{\overline{1}})+v_{m1}(c_m^\dagger c_1+c_1^\dagger c_m)\}. \tag{11}$$

A diagram representing the electronic Hamiltonian (11) is shown in Fig. 3.

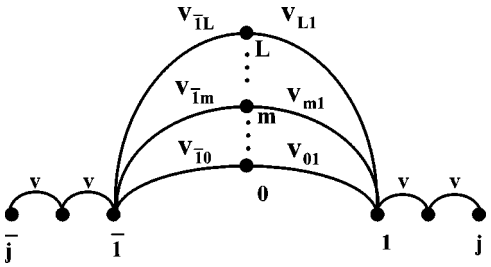

FIG. 3. Diagram representing the electronic Hamiltonian (11).

As it is well known,[26] the dominant dispersion process in polar semiconductors is due to the coupling between electrons and LO phonons.

The interaction Hamiltonian $\mathcal{H}_{int}$ has three terms

$$\mathcal{H}_{int}=\mathcal{H}_{e\text{-}e}+\mathcal{H}_{e\text{-}ph}+\mathcal{H}_{ph\text{-}ph}, \tag{12}$$

where $\mathcal{H}_{e\text{-}e}$, $\mathcal{H}_{e\text{-}ph}$ and $\mathcal{H}_{ph\text{-}ph}$ describe the electron-electron, the electron-phonon, and the phonon-phonon interactions, respectively.

$\mathcal{H}_{e\text{-}e}$ is taken in the Hartree approximation. That means that the energies ε_m of the levels in the well depend on the accumulated charge.

The electron-phonon interaction Hamiltonian has the form,

$$\mathcal{H}_{e-ph}=\sum_{\mathbf{k},\mathbf{q}_1} g_{\mathbf{k}\mathbf{q}_1}(c^\dagger_{0_{\mathbf{k}-\mathbf{q}_1}}c_{1'\mathbf{k}}b^\dagger_{1_{\mathbf{q}_1}}+c^\dagger_{1'\mathbf{k}}c_{0_{\mathbf{k}-\mathbf{q}_1}}b_{1_{\mathbf{q}_1}}). \tag{13}$$

In order to recover the translational symmetry in the xy plane we take the average on $\mathbf{q}_1$ [Ref. (1)]

$$\mathcal{H}_{e-ph}=\sum_{\mathbf{k}} g_{\mathbf{k}}(c^\dagger_{0_{\mathbf{k}}}c_{1'\mathbf{k}}b^\dagger_{1_{\mathbf{k}}}+c^\dagger_{1'\mathbf{k}}c_{0_{\mathbf{k}}}b_{1_{\mathbf{k}}}), \tag{14}$$

where $g_{\mathbf{k}}$ measure the effective strength of the interaction and was calculated as in Ref. 54.

The phonon-phonon interaction is given by[9]

$$\mathcal{H}_{ph-ph}=\sum_{\mathbf{q}_1} \gamma_{\mathbf{q}_1}(b_{1_{\mathbf{q}_1}}b^\dagger_{2_{\mathbf{q}_1}}b^\dagger_3+b^\dagger_{1_{\mathbf{q}_1}}b_{2_{\mathbf{q}_1}}b_3). \tag{15}$$

This Hamiltonian describes the decay LO$\rightarrow\widetilde{\text{LO}}+$TA and its inverse process (recombination).

As in the GaAs the TA phonons are emitted fundamentally in the [111] direction,[9] we considered here a device that was grown in this direction. The inside barrier walls act as mirrors of a Fabry-Perot interferometer selecting discrete cavity modes. These mirrors also serve for a selection of the saser modes: those running in the grown direction are reflected several times between the mirrors and stay longer in the well, while all others are lost.

With the increasing of the applied bias V, from a certain value, called saser threshold, the TA phonons associated with the cavity resonant mode, i.e., $\mathbf{q}_3=0$, stimulate strongly the LO phonon decay and their number grows sharply. Once this mode is sufficiently populated, the probability of stimulated emission for that mode exceeds the sum of the emission probabilities for all other modes. Thus, the TA phonons emit-

ted in this mode will slave the other ones, giving rise to a coherent acoustic phonon beam. This process is similar to what happens in a laser. Due to the momentum conservation $\mathbf{q}_1=\mathbf{q}_2+\mathbf{q}_3$ and because of $\mathbf{q}_3=0$ (Ref. 10) we get $\mathbf{q}_2=\mathbf{q}_1$.

The parameter $\gamma_{\mathbf{q}_1}$ appearing in Eq. (15) represents the intensity of the interaction and was estimated from Refs. 9,55 and 56.

Finally, the total Hamiltonian is the sum of both terms: the single particle and the interaction parts

$$\mathcal{H}=\sum_{\mathbf{k}} \mathcal{H}_o(\mathbf{k})+\mathcal{H}_{int}(\mathbf{k}), \tag{16}$$

where we had made the approximation that the momentum $\mathbf{q}_1$ [appearing in expressions (2), (3), and (15)]) varies in the same range as $\mathbf{k}$. We can see at expression (16) that the Hamiltonian became, in this approximation, fully uncoupled for each $\mathbf{k}$. This simplifies strongly the obtention of its solutions.

III. THE RESOLUTION OF THE HAMILTONIAN

We assume in this section that the temperature is very low. Therefore it is taken equal to zero.

In order to solve the Hamiltonian described in Sec. II we introduce the operators

$$\mathcal{O}_{j\mathbf{k}}^{n_1,n_2,n_3}=c_{j\mathbf{k}}\frac{b_{1\mathbf{k}}^{n_1}b_{2\mathbf{k}}^{n_2}b_3^{n_3}}{\sqrt{n_1!}\sqrt{n_2!}\sqrt{n_3!}}. \tag{17}$$

The operators $\mathcal{O}_{j\mathbf{k}}^{n_1,n_2,n_3^\dagger}$ create the eigenstates of $\mathcal{H}_o$ (without the hopping terms)

$$|j\mathbf{k}n_1n_2n_3\rangle\equiv\mathcal{O}_{j\mathbf{k}}^{n_1,n_2,n_3^\dagger}|0\rangle \tag{18}$$

formed by an electron at plane j and n_1 LO phonons, n_2 $\widetilde{\mathrm{LO}}$ phonons with parallel momentum $\mathbf{k}$; and n_3 TA phonons.

As it was done before, we will leave implicit the dependence on $\mathbf{k}$.

Using the operators (17) and the Hamiltonian (16) we can calculate their equations of motion. In order to simplify the notation we call $\mathbf{n}$ for the set of $\{n_1,n_2,n_3\}$ phonons

$$i\hbar\frac{d\mathcal{O}_j^{\mathbf{n}}}{dt}=[\mathcal{O}_j^{\mathbf{n}},\mathcal{H}]. \tag{19}$$

By expanding the eigenstates $|\Phi\rangle$ of $\mathcal{H}$ in the eigenstates of $\mathcal{H}_o$,

$$|\Phi\rangle=\sum_{j,\mathbf{n}} p_j^{\mathbf{n}}|j\mathbf{n}\rangle, \tag{20}$$

and due to the orthogonality of $|j\mathbf{n}\rangle$, the amplitudes can be calculated as

$$p_j^{\mathbf{n}}=\langle jn|\Phi\rangle=\langle 0|\mathcal{O}_j^{\mathbf{n}}|\Phi\rangle. \tag{21}$$

Making use of the equations turning out from Eq. (19) and the previous definition for the amplitudes, we get for $j\neq\overline{1},1,m$ $(m=0,1',2',3'\ldots L)$

$$i\hbar\frac{dp_j^{\mathbf{n}}}{dt}=\varepsilon_j^{\mathbf{n}}p_j^{\mathbf{n}}+\Upsilon_j+vp_{j+1}^{\mathbf{n}}+vp_{j-1}^{\mathbf{n}} \tag{22}$$

and for $j=\overline{1},1,m$

$$i\hbar\frac{dp_{\overline{1}}^{\mathbf{n}}}{dt}=\varepsilon_{\overline{1}}^{\mathbf{n}}p_{\overline{1}}^{\mathbf{n}}+\Upsilon_{\overline{1}}+v_{\overline{1}1'}p_{1'}^{\mathbf{n}}+v_{\overline{1}0}p_0^{\mathbf{n}}+vp_{\overline{2}}^{\mathbf{n}}+\sum_{m\geqslant 2'} v_{\overline{1}m}p_m^{\mathbf{n}}, \tag{23a}$$

$$i\hbar\frac{dp_0^{\mathbf{n}}}{dt}=\varepsilon_0^{\mathbf{n}}p_0^{\mathbf{n}}+g\sqrt{n_1}p_{1'}^{\mathbf{n}^-}+\Upsilon_0+v_{\overline{1}0}p_{\overline{1}}^{\mathbf{n}}+v_{01}p_1^{\mathbf{n}}, \tag{23b}$$

$$i\hbar\frac{dp_{1'}^{\mathbf{n}}}{dt}=\varepsilon_{1'}^{\mathbf{n}}p_{1'}^{\mathbf{n}}+g\sqrt{n_1+1}p_0^{\mathbf{n}^+}+\Upsilon_{1'}+v_{\overline{1}1'}p_{\overline{1}}^{\mathbf{n}}+v_{1'1}p_1^{\mathbf{n}}, \tag{23c}$$

$$i\hbar\frac{dp_1^{\mathbf{n}}}{dt}=\varepsilon_1^{\mathbf{n}}p_1^{\mathbf{n}}+\Upsilon_1+v_{1'1}p_{1'}^{\mathbf{n}}+v_{01}p_0^{\mathbf{n}}+vp_2^{\mathbf{n}}+\sum_{m\geqslant 2'} v_{1m}p_m^{\mathbf{n}}, \tag{23d}$$

$$i\hbar\frac{dp_m^{\mathbf{n}}}{dt}=\varepsilon_m^{\mathbf{n}}p_m^{\mathbf{n}}+v_{1m}p_1^{\mathbf{n}}+v_{\overline{1}m}p_{\overline{1}}^{\mathbf{n}}+\Upsilon_m,\quad m\geqslant 2', \tag{23e}$$

where

$$\varepsilon_j^{\mathbf{n}}=\varepsilon_j+n_1\hbar\omega_1+n_2(\hbar\omega_2-i\hbar\kappa_2)+n_3(\hbar\omega_3-i\hbar\kappa_3),$$

$$\mathbf{n}^-\equiv\{n_1-1,n_2,n_3\},$$

$$\mathbf{n}^+\equiv\{n_1+1,n_2,n_3\},$$

$$\Upsilon_j=\gamma\{\sqrt{N^-}p_j^{\mathbf{n}'}+\sqrt{N^+}p_j^{\mathbf{n}''}\},$$

$$\mathbf{n}'\equiv\{n_1-1,n_2+1,n_3+1\},$$

$$\mathbf{n}''\equiv\{n_1+1,n_2-1,n_3-1\},$$

$$N^-=n_1(n_2+1)(n_3+1),$$

$$N^+=(n_1+1)n_2n_3.$$

The amplitudes $p_j^{\mathbf{n}}$ are time dependent. We transform them

$$p_j^{\mathbf{n}}(t)=\frac{1}{\sqrt{2\pi}}\int_{-\infty}^{\infty}d\omega a_j^{\mathbf{n}}(\omega)e^{-i\omega t}. \tag{24}$$

By doing that, we get the following set of equations

$$\hbar\omega a_j^{\mathbf{n}}=\varepsilon_j^{\mathbf{n}}a_j^{\mathbf{n}}+\Gamma_j+va_{j+1}^{\mathbf{n}}+va_{j-1}^{\mathbf{n}},\quad \text{for}\quad j\neq\overline{1},1,m \tag{25a}$$

$$\hbar\omega a_1^{\mathbf{n}} = \varepsilon_1^{\mathbf{n}} a_1^{\mathbf{n}} + \Gamma_{\bar{1}} + v a_2^{\mathbf{n}} + v_{\bar{1}1'} a_{1'}^{\mathbf{n}} + v_{\bar{1}0} a_0^{\mathbf{n}} + \sum_{m \geqslant 2'} v_{\bar{1}m} a_m^{\mathbf{n}}, \tag{25b}$$

$$\hbar\omega a_0^{\mathbf{n}} = \varepsilon_0^{\mathbf{n}} a_0^{\mathbf{n}} + g\sqrt{n_1} a_{1'}^{\mathbf{n}^-} + \Gamma_0 + v_{\bar{1}0} a_{\bar{1}}^{\mathbf{n}} + v_{01} a_1^{\mathbf{n}}, \tag{25c}$$

$$\hbar\omega a_{1'}^{\mathbf{n}} = \varepsilon_{1'}^{\mathbf{n}} a_{1'}^{\mathbf{n}} + g\sqrt{n_1+1} a_0^{\mathbf{n}^+} + \Gamma_{1'} + v_{\bar{1}1'} a_{\bar{1}}^{\mathbf{n}} + v_{1'1} a_1^{\mathbf{n}}, \tag{25d}$$

$$\hbar\omega a_1^{\mathbf{n}} = \varepsilon_1^{\mathbf{n}} a_1^{\mathbf{n}} + \Gamma_1 + v a_2^{\mathbf{n}} + v_{1'1} a_{1'}^{\mathbf{n}} + v_{01} a_0^{\mathbf{n}} + \sum_{m \geqslant 2'} v_{1m} a_m^{\mathbf{n}}, \tag{25e}$$

$$\hbar\omega a_m^{\mathbf{n}} = \varepsilon_m^{\mathbf{n}} a_m^{\mathbf{n}} + \Gamma_m + v_{\bar{1}m} a_{\bar{1}}^{\mathbf{n}} + v_{1m} a_1^{\mathbf{n}}, \quad m \geqslant 2'. \tag{25f}$$

Here Γ_j is the Fourier transform of Υ_j.

In order to obtain the solutions of Eq. (25), we considered only ones three channels through which the electrons can tunnel. Such channels are the only ones that are between the bottom of the conduction band ($\varepsilon = 0$) and the Fermi energy ε_F^L at the emitter, near the resonant condition. Therefore they are the only ones that contribute significantly to the current. These channels are: one electron through the excited level and no phonons (channel 0, i.e., $\mathbf{n}=\{0,0,0\}$, one electron through the ground level and one LO phonon (channel 100), and one electron through the ground level and a pair $\widetilde{\text{LO}}$-TA phonons, respectively, (channel 011).

To solve the system above, we drop the imaginary part of $\varepsilon_j^{\mathbf{n}}$. This copes with the problems caused by the non-Hermitian Hamiltonian.

We have to note that the amplitudes a_j^0 (for $j \geqslant 1$ or $j \leqslant \overline{1}$) remain uncoupled (this tunneling channel does not mix with any other). On the other hand, the other two channels are coupled due to the ph-ph interaction. To uncouple them we propose the following transformation for the amplitudes:

$$a_j^{100} = \frac{1}{\sqrt{2}}(a_j^+ + a_j^-), \tag{26}$$

$$a_j^{011} = \frac{1}{\sqrt{2}}(a_j^+ - a_j^-). \tag{27}$$

Making the above transformations for the amplitudes a_j^{100} and a_j^{011} we get two new uncoupled channels (called channels $+$ and $-$).

Considering only the channels 0 and $\pm$, the system (25) can be rewritten as

$$v a_{j-1}^0 + (\varepsilon_j^0 - \hbar\omega) a_j^0 + v a_{j+1}^0 = 0, \tag{28a}$$

$$v a_{j-1}^{\pm} + (\varepsilon_j^{100} \pm \gamma - \hbar\omega) a_j^{\pm} + v a_{j+1}^{\pm} = 0 \quad \text{for} \quad j \neq \overline{1}, m, 1; \tag{28b}$$

$$v a_2^0 + (\varepsilon_1^0 - \hbar\omega) a_1^0 + v_{\bar{1}1'} a_{1'}^0 + \sum_{m \neq 1'} v_{\bar{1}m} a_m^0 = 0, \tag{28c}$$

$$v a_2^{\pm} + (\varepsilon_1^{100} \pm \gamma - \hbar\omega) a_1^{\pm} + v_{\bar{1}0} a_0^{\pm} + \sum_{m \neq 0} v_{\bar{1}m} a_m^{\pm} = 0, \tag{28d}$$

$$v_{1'1} a_{1'}^0 + \sum_{m \neq 1'} v_{m1} a_m^0 + (\varepsilon_1^0 - \hbar\omega) a_1^0 + v a_2^0 = 0, \tag{28e}$$

$$v_{01} a_0^{\pm} + \sum_{m \neq 1'} v_{m1} a_m^{\pm} + (\varepsilon_1^{100} \pm \gamma - \hbar\omega) a_1^{\pm} + v a_2^{\pm} = 0, \tag{28f}$$

$$v_{\bar{1}m} a_{\bar{1}}^{\pm} + (\varepsilon_m^{100} \pm \gamma - \hbar\omega) a_m^{\pm} + v_{m1} a_1^{\pm} = 0 \quad \text{for} \quad m \neq 0; \tag{28g}$$

$$v_{\bar{1}m} a_{\bar{1}}^0 + (\varepsilon_m^0 - \hbar\omega) a_m^0 + v_{m1} a_1^0 = 0 \quad \text{for} \quad m \neq 1'; \tag{28h}$$

$$v_{\bar{1}0} a_{\bar{1}}^{\pm} + (\varepsilon_0^{100} \pm \gamma - \hbar\omega) a_0^{\pm} + \frac{g}{\sqrt{2}} a_{1'}^0 + v_{01} a_1^{\pm} = 0 \tag{28i}$$

$$v_{\bar{1}1'} a_{\bar{1}}^0 + (\varepsilon_{1'}^0 - \hbar\omega) a_{1'}^0 + \frac{g}{\sqrt{2}} a_0^+ + \frac{g}{\sqrt{2}} a_0^- + v_{1'1} a_1^0 = 0. \tag{28j}$$

The amplitudes $a_m^{\pm}$ and a_m^0 appearing in equations (28) take into account the electronic energy levels different from the fundamental and excited one. To eliminate these amplitudes (the fundamental and excited levels are the only ones that participate directly in the LO phonon generation) we use the equations (28c)–(28h). The resultant system is

$$v a_{j-1}^0 + (\varepsilon_j^0 - \hbar\omega) a_j^0 + v a_{j+1}^0 = 0, \tag{29a}$$

$$v a_{j-1}^{\pm} + (\varepsilon_j^{100} \pm \gamma - \hbar\omega) a_j^{\pm} + v a_{j+1}^{\pm} = 0 \quad \text{for} \quad j \neq \overline{1}, m, 1; \tag{29b}$$

$$v a_2^0 + (\tilde{\varepsilon}_1^0 - \hbar\omega) a_1^0 + v_{\bar{1}1'} a_{1'}^0 + \tilde{v}_{\bar{1}1}^0 a_1^0 = 0, \tag{29c}$$

$$v a_2^{\pm} + (\tilde{\varepsilon}_1^{\pm} \pm \gamma - \hbar\omega) a_1^{\pm} + v_{\bar{1}0} a_0^{\pm} + \tilde{v}_{11}^{\pm} a_1^{\pm} = 0, \tag{29d}$$

$$\tilde{v}_{11}^0 a_1^0 + v_{1'1} a_{1'}^0 + (\tilde{\varepsilon}_1^0 - \hbar\omega) a_1^0 + v a_2^0 = 0, \tag{29e}$$

$$\tilde{v}_{11}^{\pm} a_1^{\pm} + v_{01} a_0^{\pm} + (\tilde{\varepsilon}_1^{\pm} \pm \gamma - \hbar\omega) a_1^{\pm} + v a_2^{\pm} = 0, \tag{29f}$$

$$v_{\bar{1}1'} a_{\bar{1}}^0 + (\varepsilon_{1'}^0 - \hbar\omega) a_{1'}^0 + \frac{g}{\sqrt{2}} a_0^+ + \frac{g}{\sqrt{2}} a_0^- + v_{1'1} a_1^0 = 0, \tag{29g}$$

$$v_{\bar{1}0} a_{\bar{1}}^{\pm} + (\varepsilon_0^{100} \pm \gamma - \hbar\omega) a_0^{\pm} + \frac{g}{\sqrt{2}} a_{1'}^0 + v_{01} a_1^{\pm} = 0, \tag{29h}$$

where

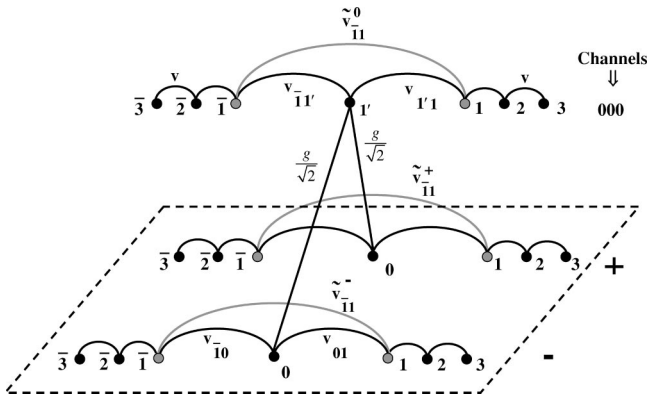

FIG. 4. Diagram representing equations (29). The vertical transition represents the LO phonon emission (absorption). As the channels + and − have the same energy, they are represented in the same plane. The gray points represent the sites with the renormalized energies and the gray lines are the renormalized hoppings.

$$\tilde{v}^{0}_{\bar{1}1}=\sum_{m\neq 1'}\frac{v_{\bar{1}m}v_{m1}}{(\hbar\omega-\varepsilon^{0}_{m})} \tag{30}$$

and

$$\tilde{v}^{\pm}_{\bar{1}1}=\sum_{m\neq 0}\frac{v_{\bar{1}m}v_{m1}}{(\hbar\omega-\varepsilon^{100}_{m}\mp\gamma)} \tag{31}$$

are renormalized hoppings joining sites $j=\bar{1},1$, and

$$\tilde{\varepsilon}^{0}_{\bar{1}}=\varepsilon^{0}_{\bar{1}}+\Sigma^{0}_{\bar{1}}, \tag{32a}$$

$$\tilde{\varepsilon}^{\pm}_{\bar{1}}=\varepsilon^{100}_{\bar{1}}+\Sigma^{\pm}_{\bar{1}}, \tag{32b}$$

$$\tilde{\varepsilon}^{0}_{1}=\varepsilon^{0}_{1}+\Sigma^{0}_{1}, \tag{32c}$$

$$\tilde{\varepsilon}^{\pm}_{1}=\varepsilon^{100}_{1}+\Sigma^{\pm}_{1}, \tag{32d}$$

are renormalized energies at the sites $j=\bar{1},1$ for each channel, where

$$\Sigma^{0}_{\bar{1}}=\sum_{m\neq 1'}\frac{v^{2}_{\bar{1}m}}{(\hbar\omega-\varepsilon^{0}_{m})} \tag{33a}$$

$$\Sigma^{\pm}_{\bar{1}}=\sum_{m\neq 0}\frac{v^{2}_{\bar{1}m}}{(\hbar\omega-\varepsilon^{100}_{m}\mp\gamma)} \tag{33b}$$

$$\Sigma^{0}_{1}=\sum_{m\neq 1'}\frac{v^{2}_{m1}}{(\hbar\omega-\varepsilon^{0}_{m})} \tag{33c}$$

$$\Sigma^{\pm}_{1}=\sum_{m\neq 0}\frac{v^{2}_{m1}}{(\hbar\omega-\varepsilon^{100}_{m}\mp\gamma)}. \tag{33d}$$

A diagram representing equations (29) is shown in Fig. 4. To solve the system (29) we proceed as follows.

For the channel 0 and ±, in the region $j\geqslant 1$ the solutions of (29a) and (29b) are, respectively,

$$a^{0}_{j}=A^{0}_{T}e^{ik'_{0}z_{j}}, \tag{34}$$

$$a^{\pm}_{j}=A^{\pm}_{T}e^{ik^{\pm}z_{j}}, \tag{35}$$

where z_j is the coordinate of the plane j ($z_j=ja$; a is the lattice parameter), A^{0}_{T}, $A^{\pm}_{T}$ are the amplitudes of the transmitted wave, and k'_0 and $k^{\pm}$ are the z component of the wave vectors that fulfills the dispersion relation

$$\hbar\omega=\varepsilon^{0}_{1}+2v\cos(k'_{0}a), \tag{36}$$

$$\hbar\omega=\varepsilon^{100}_{1}+2v\cos(k^{\pm}a)\pm\gamma. \tag{37}$$

We did not consider the terms $e^{-ik'_{\mathbf{n}}z_j}$ because we assume that there are no electrons coming in from the right of the DBH.

In the region $j\leqslant -1$ we have two kinds of solutions. The first one is obtained for the excited level that is above the bottom of the conduction band, in this case the solution is

$$a^{0}_{j}=A_{R}e^{-ik_{0}z_{j}}+A_{I}e^{ik_{0}z_{j}} \tag{38}$$

where A_R and A_I are the amplitudes of the reflected and incident waves and k_0 satisfies

$$\hbar\omega=\varepsilon^{0}_{1}+2v\cos(k_{0}a). \tag{39}$$

The second kind of solution is obtained for the ground state that is below the bottom of the conduction band then, in this case, the solutions are evanescent modes with amplitudes A^{+}_{E} and A^{-}_{E}

$$a^{\pm}_{j}=A^{\pm}_{E}e^{\kappa^{\pm}z_{j}} \tag{40}$$

where the $\kappa^{\pm}$ are positive and fulfill the relations

$$\hbar\omega=\varepsilon^{100}_{\bar{1}}+2v\cosh(\kappa^{\pm}a)\pm\gamma. \tag{41}$$

After replacing Eqs. (34), (35), (38), and (40) in Eq. (29) we get a system of nine equations with the following nine unknown quantities:

$$a^{0}_{1'},\quad a^{+}_{0},\quad a^{-}_{0},\quad A_{R},\quad A^{0}_{T},\quad A^{-}_{E},\quad A^{+}_{E},\quad A^{-}_{T},$$
$$\text{and}\quad A^{+}_{T}.$$

The solution of this system permits to calculate the electronic current taking into account the e-ph and ph-ph interactions and to obtain a set of five kinetic equations as it is shown in the following section.

IV. THE KINETIC EQUATIONS

To get the kinetic equations that describe the population of electrons and phonons we need to obtain the equations of motion for the electron number operators $c^{\dagger}_{j}c_{j}$ and the phonon number operators $b^{\dagger}_{i}b_{i}$

$$i\hbar\frac{d}{dt}(c_j^\dagger c_j)=[c_j^\dagger c_j,\mathcal{H}],\quad i\hbar\frac{d}{dt}(b_i^\dagger b_i)=[b_i^\dagger b_i,\mathcal{H}]. \tag{42}$$

We define the average populations for electrons in the excited and ground states as

$$\overline{n_j}=\sum_{occ}\langle\Phi|c_j^\dagger c_j|\Phi\rangle \quad \text{for} \quad j=0,\ 1'.$$

From the definition (20) of $|\Phi\rangle$, the electrons average populations can be calculated as

$$\overline{n_j}=\sum_{\mathbf{n},occ}|p_j^{\mathbf{n}}|^2 \tag{43}$$

For the LO, $\widetilde{\text{LO}}$, and TA phonons, the average populations are

$$\overline{n_i}=\sum_{occ}\langle\Phi|b_i^\dagger b_i|\Phi\rangle=\sum_{\mathbf{n},occ,j}|p_j^{\mathbf{n}}|^2 n_i \quad \text{for} \quad i=1,2,3. \tag{44}$$

Using the equations (42) we get the set of quantum kinetic equations

$$\frac{d\overline{n_{1'}}}{dt}=G^I_{1'}-G^O_{1'}-G^E_{1'}, \tag{45a}$$

$$\frac{d\overline{n_0}}{dt}=G^I_0-G^O_0+G^E_{1'}, \tag{45b}$$

$$\frac{d\overline{n_1}}{dt}=G^E_{1'}-G^E_{\text{LO}}, \tag{45c}$$

$$\frac{d\overline{n_2}}{dt}=G^E_{\text{LO}}-D_{\widetilde{\text{LO}}}, \tag{45d}$$

$$\frac{d\overline{n_3}}{dt}=G^E_{\text{LO}}-E_{TA}, \tag{45e}$$

where

$$G^I_{1'}=\frac{2}{\hbar}\sum_{\mathbf{n},occ}v_{\overline{1}1'}\text{Im}\{p_{1'}^{\mathbf{n}*}p_{\overline{1}}^{\mathbf{n}}\} \tag{46}$$

is the electronic input rate from the emitter to the excited level;

$$G^O_{1'}=\frac{2}{\hbar}\sum_{\mathbf{n},occ}v_{1'1}\text{Im}\{p_1^{\mathbf{n}*}p_{1'}^{\mathbf{n}},\} \tag{47}$$

is the output rate from there to the collector.

$$G^E_{1'}=\frac{2}{\hbar}\sum_{\mathbf{n},occ}g\ \text{Im}\{p_0^{\mathbf{n}^+*}p_{1'}^{\mathbf{n}},\}\sqrt{n_1+1}, \tag{48}$$

represents the net balance between emission and absorption of LO phonons via electron transitions:

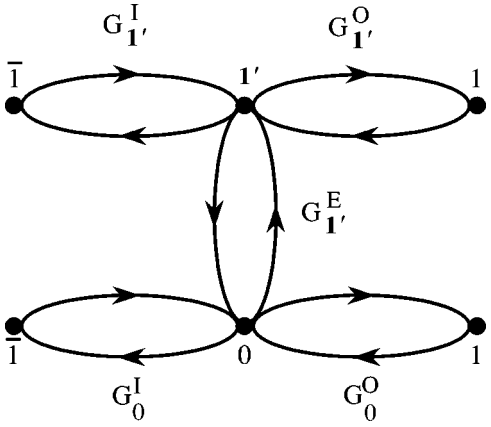

FIG. 5. Diagram for the several rates appearing in Eqs. (41a) and (41b).

$$G^I_0=\frac{2}{\hbar}\sum_{\mathbf{n},occ}v_{\overline{1}0}\text{Im}\{p_0^{\mathbf{n}*}p_{\overline{1}}^{\mathbf{n}}\} \tag{49}$$

is the input rate from the emitter directly to the ground state, and

$$G^O_0=\frac{2}{\hbar}\sum_{\mathbf{n},occ}v_{01}\text{Im}\{p_1^{\mathbf{n}*}p_0^{\mathbf{n}}\} \tag{50}$$

stands for the output rate from the ground state to the collector.

The balance between the decay of one phonon LO by emission of a pair of $\widetilde{\text{LO}}$ and TA phonons, and its inverse process (i.e., recombination) is given by

$$G^E_{\text{LO}}=\frac{2}{\hbar}\sum_{\mathbf{n},occ}\gamma\ \text{Im}\{p_j^{\mathbf{n}^+*}p_j^{\mathbf{n}^-}\}\sqrt{N}, \tag{51}$$

where $N\equiv(n_1+1)(n_2+1)(n_3+1)$.

The decay rate of the $\widetilde{\text{LO}}$ population turns out to be

$$D_{\widetilde{\text{LO}}}=2\kappa_2\sum_{\mathbf{n},j}\{p_j^{\mathbf{n}*}p_j^{\mathbf{n}}\}n_2=2\kappa_2\overline{n_2}. \tag{52}$$

Finally the escape rate of the TA phonons is given by

$$E_{TA}=2\kappa_3\sum_{\mathbf{n},j}\{p_j^{\mathbf{n}*}p_j^{\mathbf{n}}\}n_3=2\kappa_3\overline{n_3}. \tag{53}$$

A diagram for the input and output electron rates is shown in Fig. 5.

The kinetic equations (45) can be approximated by a system involving only populations. To do that we have to replace the amplitudes $p_j^{\mathbf{n}}$ from Eqs. (22) and (23) (See the Appendix for a detailed calculation). Then, we get a new set of kinetic equations

$$\frac{d\overline{n_{1'}}}{dt}=G-R_{1'}\overline{n_{1'}}-R_w, \tag{54a}$$

$$\frac{d\overline{n_0}}{dt}=-R_0\overline{n_0}+R_w, \tag{54b}$$

$$\frac{d\overline{n_1}}{dt} = R_w - R_\gamma, \tag{54c}$$

$$\frac{d\overline{n_2}}{dt} = -\kappa_2 \overline{n_2} + R_\gamma, \tag{54d}$$

$$\frac{d\overline{n_3}}{dt} = -\kappa_3 \overline{n_3} + R_\gamma, \tag{54e}$$

where

$$R_w = w[\overline{n_1}'(\overline{n_1}+1) - \overline{n_0}\,\overline{n_1}], \tag{55}$$

$$R_\gamma = \gamma_o[\overline{n_1}(\overline{n_2}+1)(\overline{n_3}+1) - (\overline{n_1}+1)\overline{n_2}\ \ \overline{n_3}]. \tag{56}$$

G is the input current, R_1' and R_0 are the escape rates for one electron through the right barrier and w is the transition rate due to LO phonon emission estimated in the Appendix (and more roughly in Ref. 1). The other parameters are: the decay rate of a LO phonon γ_o, the decay rate of a $\widetilde{\text{LO}}$ phonon κ_2 and the TA phonon escape rate κ_3.

It can be seen in the expressions (55) and (56) that the Bose factors were obtained. That means that the phonons are produced in a stimulated regime. For the case of TA phonons, the Bose factor $\overline{n_3}+1$ is thousands times greater than the others.

V. RESULTS AND CONCLUSIONS

The results presented here correspond only to the stationary case, i.e., $p_j^{\mathbf{n}}(t) = a_j^{\mathbf{n}}(\omega)e^{i\omega t}$. In this case, all the populations (43) and (44), and the rates (46)–(53) are time independent and they can be written as the same expressions of $a_j^{\mathbf{n}}(\omega)$ instead of $p_j^{\mathbf{n}}(t)$. The amplitudes $a_j^{\mathbf{n}}(\omega)$ are the solutions of the system (29).

The following parameters were used in our calculations. The barriers are 42.4 Å wide and 300 meV high (38% of Al concentration). The well has a width of 203.4 Å. The Fermi energy at the emitter was fixed at 15 meV. The values estimated for the decay rate κ_2 and the escape rate κ_3 were 30 ps^{-1} and 0.05 ps^{-1}, respectively. The other parameters used are: w, that depends on the applied bias but it is of the order of 2.5 ps^{-1}, $\gamma_o = 0.11$ ps^{-1} taken from Ref. 9, and g, that also depends on the applied bias and is of the order of 3.2 ps^{-1}. The value of γ was taken equal to 0.65 meV and was calculated from the experimental value of γ_o using Refs. 55 and 56.

The transmittance through the DBH is calculated from

$$T = \frac{|A_T^0|^2 + |A_T^+|^2 + |A_T^-|^2}{|A_I|^2}. \tag{57}$$

A plot of the transmittance as a function of energy is shown in Fig. 6. It can be seen that when the ph-ph interaction is considered (taking $\gamma \neq 0$), a central peak appears. The other two peaks correspond to the polaronic branches already shown in previous works.[57,58]

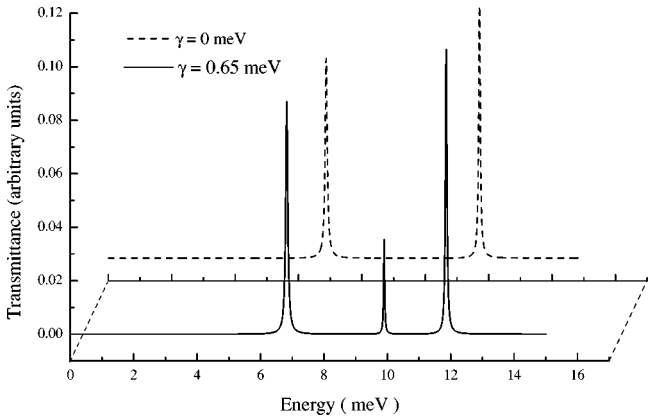

FIG. 6. Dashed line: the two polaronic peaks when $\gamma = 0$. Solid line: if we assume $\gamma \neq 0$, it appears a third peak corresponding mainly to one electron in the ground state with a pair $(\widetilde{\text{LO}} + \text{TA})$ of phonons.

Once the transmission probabilities through each channel are obtained, the output electronic current (equal to the input current at the stationary regime) through the structure can be calculated by summing over the occupied states at the emitter. This sum can be easily transformed into the integral

$$G(V) = \frac{S}{2\pi^2}\frac{m^*}{\hbar^3}\int_0^{\varepsilon_F^L} \frac{(\varepsilon_F^L - \varepsilon) j(\varepsilon)\rho(\varepsilon)}{1+R+T} d\varepsilon \tag{58}$$

where $S = 0.5 \times 10^{-3}$ mm^2 is the device area, $m^* = 0.067 m_e$ is the effective electron mass, R is the reflectance and

$$j(\varepsilon) = \frac{4v}{\hbar}\frac{1}{|A_I|^2}\{|A_T^0|^2 \sin(k_0' a) + |A_T^+|^2 \sin(k^+ a) + |A_T^-|^2 \sin(k^- a)\},$$

$$\rho(E) = \frac{1}{2v\,\sin(k_0 a)}.$$

Instead of using the expression (58) to calculate the electronic current G, it is calculated from the sum of the terms (46) and (49).

The difference between the currents calculated for $\gamma \neq 0$ and $\gamma = 0$ is appreciable only in the dashed region of Fig. 7, that is amplified in the inset.

Finally, the saser intensity and the TA phonon population are shown in Fig. 8. This curve is obtained by solving the kinetic equations (54).

We can see in Fig. 8 that the intensity of the beam follows the current. Therefore the saser signal diminishes when the system goes out of resonance.

In a previous paper[10] we showed that the coherent stimulated emission occurs when primary LO phonon injection G_1 is greater than $\Gamma_1 \kappa_2 \kappa_3 / \gamma^2$, where the injection rate G_1 is defined as $G_1 = w\overline{n_1}'$ and the absorption rate Γ_1 is defined as $\Gamma_1 = w(\overline{n_0} - \overline{n_1}')$.

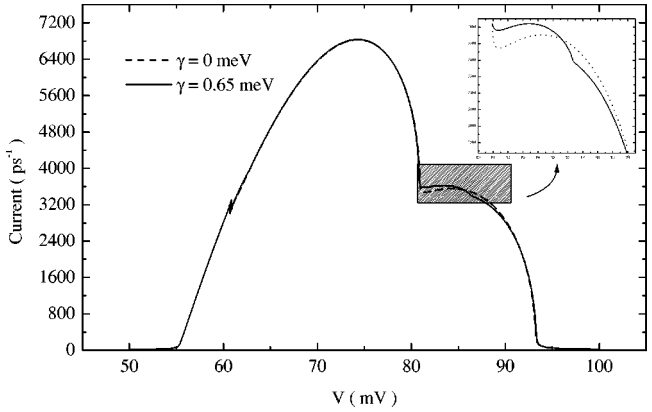

FIG. 7. Solid line: the current for $\gamma \neq 0$. For comparison, the electronic current when $\gamma = 0$ is shown in the inset (dashed line). It appears a shoulder in G $(\gamma \neq 0)$ corresponding to the third peak of Fig. 6. The cross-sectional area used was $S = 0.5 \times 10^{-3}$ mm^2.

For the parameters used here, this condition occurs when V is greater than $V_{th_1} = 60.25$ meV and less than $V_{th_2} = 94.04$ meV whereas the incoherent TA emission begins at $V = 60.18$ meV and does not finish so sharply because the tail of the peak corresponding to the excited electron state remains above the bottom of the conduction band at the emitter.

At the beginning of the LO phonon emission the electrons begin to accumulate in the ground state of the well for which the escape rate is low. Therefore the accumulated charge repels the input of new electrons. That means that the levels in the well tend to rise and to diminish their energy difference, preventing the LO phonon emission.

The process described above represents an instability that was discussed in detail in a previous paper.[58] Due to this process, at the beginning of the phonon emission, undamped temporal oscillations appear, meaning that, in this region, stationary solutions do not exist. In consequence, the self-consistent treatment of the charge accumulation, oscillating between two branches does not converge. This can be seen in Fig. 8 as a thick vertical line, due to the overlap of the oscillations.

The total input (pump) power injected in the form of electrons, is given by the product $G \times (\mathrm{eV})$ that is proportional to the device cross-sectional area S, whereas the power of the saser beam is given by $(\kappa_3 \overline{n_3}) \times (\hbar \omega_3)$. Since, at the stationary state, $\kappa_3 \overline{n_3} = R_0 \overline{n_0}$, and $G = R_0 \overline{n_0} + R_{1'} \overline{n_{1'}}$, the power conversion efficiency is

$$\eta = \left(\frac{R_0 \overline{n_0}}{R_0 \overline{n_0} + R_{1'} \overline{n_{1'}}} \right) \left(\frac{\hbar \omega_3}{\mathrm{eV}} \right)$$

This efficiency is of the order of 1%.

The internal quantum efficiency of our device, i.e., the relation between coherent and incoherent phonons, is taken in this paper to be equal to one, because it is supposed that, above the threshold, the coherent mode slaves all the others.[10]

In conclusion we presented here a full-quantum many-body formalism to study the GaAs-$Al_xGa_{1-x}As$ double-barrier heterostructure phonon laser. The Hamiltonian considered takes into account explicitly the electrons, the three phonon branches, the electron-phonon interaction, and the phonon-phonon interaction. The electron-electron interaction inside the well was treated in the Hartree approximation. The electronic part of the Hamiltonian is solved exactly through the renormalization procedure that takes into account all the electronic levels in the well. The main approximation done to solve this many-body problem was to take an average over the transversal (parallel to the interfaces) momenta, in order to recover the translational symmetry.

Besides, a set of quantum kinetic equations were deduced. This set is different from those presented in a previous work[1] where the kinetic equations were derived phenomenologically. We can see that the results obtained using the old kinetic equations are qualitatively similar to those presented here. In fact, the old kinetic equations could be derived as approximations of the quantum ones. These approximations, showed in the Appendix, seem to be rather rough. We neglected crossed terms and did some averages. It was shown that when the phonon-phonon interaction is considered, only small modifications are observed for the current.

In summary, the accurate full-quantum calculations for a

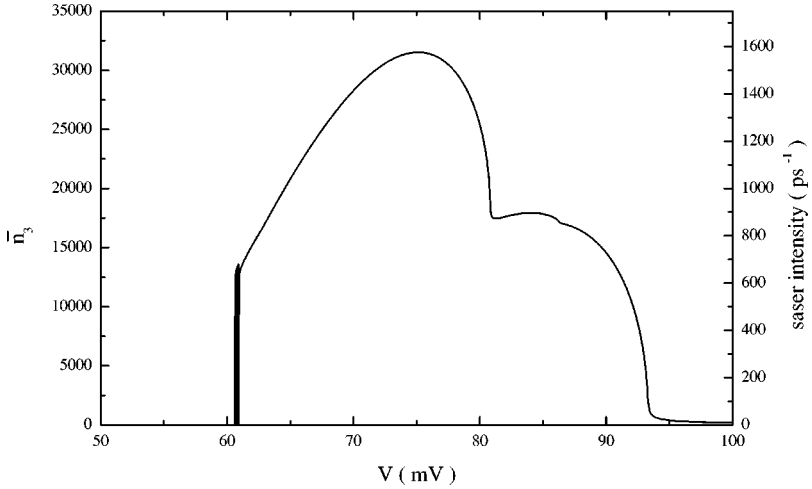

FIG. 8. The TA phonon population $\overline{n_3}$ and the saser intensity $S = \kappa_3 \overline{n_3}$.

DBH phonon laser confirm the results obtained using rougher phenomenological methods.[1]

ACKNOWLEDGMENT

One of us (I.C.) wants to acknowledge Latin American agency CLAF for financial support.

APPENDIX

In this appendix, we will show the way to obtain each term of equations (54) from Eq. (45). To illustrate the procedure, we will limit ourselves to showing only two examples.

We begin with the term

$$G_{1'}^{O}=\frac{2}{\hbar}\sum_{\mathbf{n},\mathrm{occ}} v_{1'1}\mathrm{Im}\{p_1^{\mathbf{n}*}p_{1'}^{\mathbf{n}}\}. \tag{A1}$$

The channel 000 is the only one that contributes significantly to the sum appearing in Eq. (A1) (see Figs. 3 and 4). Taking this into account, the expression (A1) can be rewritten as

$$G_{1'}^{O}=\frac{2}{\hbar}\sum_{\mathrm{occ}} v_{1'1}\mathrm{Im}\{p_1^{0*}p_{1'}^{0}\}. \tag{A2}$$

As the amplitudes appearing in Eq. (A2) are time dependent, we substitute one of them by their Fourier transform using Eq. (24)

$$\mathrm{Im}\{p_1^{0*}p_{1'}^{0}\}=\mathrm{Im}\left\{\frac{1}{\sqrt{2\pi}}\int_{-\infty}^{\infty}d\omega a_1^{0*}(\omega)e^{i\omega t}p_{1'}^{0}\right\}. \tag{A3}$$

To obtain an expression for the amplitude $a_1^{0*}(\omega)$, we use Eq. (29e) and neglect the term containing the renormalized hopping $\tilde{v}_{11}^{0}$ in it. Taking into account the dispersion relation (36) and (32c) and using Eq. (34) to calculate the amplitude in the plane $j=2$, we get

$$a_1^{0*}(\omega)=\Xi_{1'1}a_{1'}^{0*}(\omega), \tag{A4}$$

where

$$\Xi_{1'1}=v_{1'1}\frac{(\Sigma_1^0-ve^{-ik_0'a})}{[\Sigma_1^{0^2}-2v\Sigma_1^0\cos(k_0'a)+v^2]}.$$

Replacing Eq. (A4) in Eq. (A3)

$$\mathrm{Im}\{p_1^{0*}p_{1'}^{0}\}=\frac{1}{\sqrt{2\pi}}\mathrm{Im}\left\{\int_{-\infty}^{\infty}\Xi_{1'1}a_{1'}^{0*}(\omega)d\omega e^{i\omega t}p_{1'}^{0}\right\}. \tag{A5}$$

The term $\Xi_{1'1}$ inside the integral varies very slowly in the range where the amplitude $a_{1'}^{0*}(\omega)$ is not null. Therefore we can take it out of the integral. Now, performing the integral over ω and taking the imaginary part we get

$$G_{1'}^{O}=\frac{2}{\hbar}\sum_{occ} v_{1'1}^2\frac{v}{[\Sigma_1^{0^2}-2v\Sigma_1^0\cos(k_0'a)+v^2]}\sin(k_0'a)|p_{1'}^{0}|^2. \tag{A6}$$

Defining $\overline{n}_{1'}\equiv\Sigma_{occ}|p_{1'}^{0}|^2$ we get

$$G_{1'}^{O}=R_{1'}\overline{n}_{1'},$$

where

$$R_{1'}=\frac{2}{\hbar}v_{1'1}^2\frac{v}{[\Sigma_1^{0^2}-2v\Sigma_1^0\cos(k_0'a)+v^2]}\sin(k_0'a).$$

When the renormalization effects are not taken into account, i.e., $\Sigma_1^0=0$, the expression obtained here for $R_{1'}$ is the same as that appearing in Ref. 59.

The other term to be analyzed here is the rate of LO phonon emission (48)

$$G_{1'}^{E}=\frac{2}{\hbar}\sum_{\mathbf{n},occ} g\ \mathrm{Im}\{p_0^{\mathbf{n}^+*}p_{1'}^{\mathbf{n}}\}\sqrt{n_1+1}. \tag{A7}$$

First, we expand the term inside the sum and change the range over which the n_1 runs to obtain Eq. (55). That is,

$$\sum_{\mathbf{n}}\mathrm{Im}\{p_0^{\mathbf{n}^+*}p_{1'}^{\mathbf{n}}\}\sqrt{n_1+1}=\sum_{\mathbf{n}} i(p_0^{(n_1+1)n_2n_3^*}p_{1'}^{\mathbf{n}}\sqrt{n_1+1}-p_{1'}^{(n_1-1)n_2n_3^*}p_0^{\mathbf{n}}\sqrt{n_1}). \tag{A8}$$

Writing $p_0^{(n_1+1)n_2n_3^*}$ in the first term of Eq. (A8) in terms of its Fourier transform $a_0^{(n_1+1)n_2n_3^*}$, doing the same with $p_{1'}^{(n_1-1)n_2n_3^*}$ in the second term and using Eqs. (25c) and (25d) (only the terms that contain the factor g) we get

$$a_0^{(n_1+1)n_2n_3}=\frac{g}{\Delta_0^{(n_1+1)n_2n_3}}\sqrt{n_1+1}a_{1'}^{\mathbf{n}}, \tag{A9}$$

and

$$a_{1'}^{(n_1-1)n_2n_3}=\frac{g}{\Delta_{1'}^{(n_1-1)n_2n_3}}\sqrt{n_1}a_0^{\mathbf{n}}, \tag{A10}$$

where

$$\Delta_0^{(n_1+1)n_2n_3}=\hbar\omega-(n_1+1)\hbar\omega_1-n_2\hbar\omega_2-n_3\hbar\omega_3-\varepsilon_0$$

and

$$\Delta_{1'}^{(n_1-1)n_2n_3}=\hbar\omega-(n_1-1)\hbar\omega_1-n_2\hbar\omega_2-n_3\hbar\omega_3-\varepsilon_{1'}.$$

Replacing Eqs. (A9) and (A10) in Eq. (A7) and doing the inverse Fourier transform for the amplitudes with the same approximation as those made to get equation (A6)

$$G^E_{1'}=\sum_{\mathbf{n},occ}\left\{\frac{g^2}{\hbar\Delta_0^{(n_1+1)n_2n_3}}(n_1+1)\left|p^{\mathbf{n}}_{1'}\right|^2 - \frac{g^2}{\hbar\Delta_{1'}^{(n_1-1)n_2n_3}}n_1\left|p^{\mathbf{n}}_0\right|^2\right\}. \tag{A11}$$

If we do now a mean-field approximation to take the phonon terms out of the sums, we get the following expression

$$G^E_{1'}=(\overline{n}_1+1)\sum_{\mathbf{n},occ}\frac{g^2}{\hbar\Delta_0^{(n_1+1)n_2n_3}}|p^{\mathbf{n}}_{1'}|^2 - \overline{n}_1\sum_{\mathbf{n},occ}\frac{g^2}{\hbar\Delta_{1'}^{(n_1-1)n_2n_3}}|p^{\mathbf{n}}_0|^2. \tag{A12}$$

The amplitudes $p^{000}_{1'}$ and p^{100}_0 are the only ones that contribute significantly to the first and second sum, respectively. Taking this into account and the fact that close to the resonance $(\varepsilon_{1'}-\varepsilon_0\simeq\hbar\omega_1)$ $\Delta^0_{1'}\simeq\Delta^{100}_0=\Delta$, equation (A12) can be written as

$$G^E_{1'}=(\overline{n}_1+1)\sum_{occ}\frac{g^2}{\hbar\Delta}|p^0_{1'}|^2-\overline{n}_1\sum_{occ}\frac{g^2}{\hbar\Delta}|p^{100}_0|^2. \tag{A13}$$

Finally the expression (A13) can be written as

$$G^E_{1'}\simeq w[\overline{n}_{1'}(\overline{n}_1+1)-\overline{n}_0\ \overline{n}_1]\equiv R_w, \tag{A14}$$

where

$$w=\sum_{occ}\frac{g^2}{\hbar\Delta},$$

$$\overline{n}_0\equiv\sum_{occ}|p^{100}_0|^2 \quad\text{and}\quad \overline{n}_{1'}\equiv\sum_{occ}|p^0_{1'}|^2.$$

The other terms appearing in Eq. (45) can be transformed by the same procedure described above.

In summary, to obtain the kinetic equations similar to that used in Ref. 1 i.e., involving only populations, we did not take into account the crossed terms. For example, if we consider the term with $v_{\overline{10}}$ in Eq. (25c) to obtain Eq. (A9), then the expression for the amplitude $a_0^{(n_1+1)n_2n_3}$ would have a term depending on $v_{\overline{10}}$. That term would describe a virtual process. In this process, an electron tunnels through the left barrier $(j=\overline{1})$ directly to the ground state $(j=0)$ emitting one LO phonon. Even when this process could occur, its probability is much smaller than that of the indirect process: first tunnel to the excited level, and then decay to the ground state emitting a LO phonon. Therefore we make the sum of each process as being independent. The results obtained from equations (54) are quite similar to those obtained from Eq. (45).

[1] S. S. Makler, M. I. Vasilevskiy, E. V. Anda, D. E. Tuyarot, J. Weberszpil, and H. M. Pastawski, J. Phys.: Condens. Matter **10**, 5905 (1998).
[2] L. L. Chang, L. Esaki, and R. Tsu, Appl. Phys. Lett. **24**, 593 (1974).
[3] F. Capasso and S. Datta, Phys. Today **43** (2), 74 (1990).
[4] V. J. Goldman, D. C. Tsui, and J. E. Cunningham, Phys. Rev. Lett. **58**, 1256 (1987).
[5] V. J. Goldman, D. C. Tsui, and J. E. Cunningham, Phys. Rev. B **36**, 7635 (1987).
[6] B. Jusserand, F. Mallot, J. M. Moison, and G. Leroux, Appl. Phys. Lett. **57**, 560 (1990).
[7] J. M. Jacob, D. M. Kim, A. Bouchalkha, J. J. Sony, J. F. Klem, H. Hou, C. W. Tu, and H. Morkoç, Solid State Commun. **91**, 721 (1994).
[8] F. Vallée and F. Bogani, Phys. Rev. B **43**, 12 049 (1991).
[9] F. Vallée, Phys. Rev. B **49**, 2460 (1994).
[10] I. Camps and S. S. Makler, Solid State Commun. **116**, 191 (2000).
[11] H. Haken, Rev. Mod. Phys. **47**, 67 (1975).
[12] H. Haken, in *Synergetics*, 3rd ed., edited by H. Haken, Springer Series in Synergetics, (Springer-Verlag, Berlin, 1983).
[13] C. L. Tang, Phys. Rev. **134**, A1166 (1964).
[14] E. B. Tucker, Phys. Rev. Lett. **6**, 547 (1961).
[15] J. A. Giordmaine and W. Kaiser, Phys. Rev. **144**, 676 (1966).
[16] E. Garmire, F. Pandarese, and C. H. Townes, Phys. Rev. B **11**, 160 (1963).
[17] G. C. Cho, W. Kutt, and H. Kurz, Phys. Rev. Lett. **65**, 764 (1990).
[18] T. K. Cheng, J. Vidal, H. J. Zeiger, G. Dresselhaus, M. S. Dresselhaus, and E. P. Ippen, Appl. Phys. Lett. **59**, 1923 (1991).
[19] T. Pfeifer, W. Kutt, H. Kurz, and R. Scholz, Phys. Rev. Lett. **69**, 3248 (1992).
[20] W. Kutt, G. C. Cho, T. Pfeifer, and H. Kurz, Semicond. Sci. Technol. **7**, b77 (1992).
[21] W. Albrecht, T. Kruse, and H. Kurz, Phys. Rev. Lett. **69**, 1451 (1992).
[22] W. A. Kutt, W. Albrecht, and H. Kurz, IEEE J. Quantum Electron. **28**, 2434 (1992).
[23] R. Merlin, Solid State Commun. **102**, 207 (1997).
[24] P. Basseras, S. M. Gracewski, G. W. Wicks, and R. J. D. Miller, J. Appl. Phys. **75**, 2761 (1994).
[25] E. P. N. Damen, A. F. M. Arts, and H. W. de Wijn, Phys. Rev. Lett. **74**, 4249 (1995).
[26] H. Haken, *Quantum Field Theory of Solids. An Introduction* (North-Holland, Amsterdam, 1976), p. 218.
[27] W. E. Bron and W. Grill, Phys. Rev. Lett. **40**, 1459 (1978).
[28] J. Y. Prieur, R. Höhler, J. Joffrin, and M. Devaud, Europhys. Lett. **24**, 409 (1993).
[29] J. Y. Prieur, M. Devaud, J. Joffrin, C. Barre, and M. Stenger, Physica B **220**, 235 (1996).
[30] S. T. Zavtrak, Phys. Rev. E **51**, 2480 (1995).
[31] S. T. Zavtrak, Phys. Rev. E **51**, 3767 (1995).
[32] S. T. Zavtrak, Zh. Tekh. Fiz. **65**, 123 (1995).

[33] S. T. Zavtrak, J. Acoust. Soc. Am. **99**, 730 (1996).
[34] A. A. Doinikov and S. T. Zavtrak, J. Acoust. Soc. Am. **99**, 3849 (1996).
[35] S. T. Zavtrak and I. V. Volkov, Tech. Phys. **42**, 406 (1997).
[36] P. A. Fokker, J. I. Dijkhuis, and H. W. de Wijn, Phys. Rev. B **55**, 2925 (1997).
[37] P. A. Fokker, R. S. Meltzer, Y. P. Wang, J. I. Dijkhuis, and H. W. de Wijn, Phys. Rev. B **55**, 2934 (1997).
[38] W. Guang-Yu, Nucl. Sci. Technol. **7**, 40 (1996).
[39] W. Guangyu, Nuc. Soc. China **7**, 295 (1995).
[40] J. C. Solem and G. C. Baldwin, Nuovo Cimento Soc. Ital. Fis., **17D**, 1131 (1995).
[41] M. R. Andrews, C. G. Townsend, H. J. Miesner, D. S. Durfee, D. M. Kurn, and W. Ketterle, Science **275**, 637 (1997).
[42] H. J. Miesner, D. Stamper-Kurn, M. R. Andrews, D. S. Durfee, S. Inouye, and W. Ketterle, Science **279**, 1005 (1998).
[43] E. A. Burt, R. W. Ghrist, C. J. Myatt, M. J. Holland, E. A. Cornell, and C. E. Wieman, Phys. Rev. Lett. **79**, 337 (1997).
[44] M. Yasuda and F. Shimizu, Phys. Rev. Lett. **77**, 3090 (1996).
[45] S. Wallentowitz, W. Vogel, I. Siemers, and P. E. Toschek, Phys. Rev. A **54**, 943 (1996).
[46] D. Kleppner, Phys. Today **50** (8), 11 (1997).
[47] Z. L. Yu and S. Boseck, Rev. Mod. Phys. **67**, 863 (1995).
[48] R. S. Gilmore, J. Phys. D **29**, 1389 (1996).
[49] H. Maris, Sci. Am. **278** (1), 64 (1998).
[50] Z. H. Chang, A. Rundquist, H. W. Wang, I. C. M. M. Murnane, and H. C. Kapteyn, IEEE J. Sel. Top. Quantum Electron. **4**, 266 (1998).
[51] A. Rundquist, C. G. Durfee, Z. H. Chang, C. Herne, S. Backus, M. M. Murnane, and H. C. Kapteyn, Science **280**, 1412 (1998).
[52] M. E. Msall, A. Klimashov, S. Kronmüller, H. Kostial, W. Dietsche, and K. Friedland, Appl. Phys. Lett. **74**, 821 (1999).
[53] J. P. Wolfe, *Imaging Phonons: Acoustic Wave Propagation in Solids* (Cambridge University Press, Cambridge, 1998).
[54] G. Weber and J. F. Ryan, Phys. Rev. B **45**, 11 202 (1992).
[55] P. G. Klemens, Phys. Rev. **148**, 845 (1966).
[56] J. M. Ziman, *Electrons and Phonons. The Theory of Transport Phenomena in Solids* (Oxford University Press, Oxford, 1972).
[57] D. E. Tuyarot, S. S. Makler, E. V. Anda, and M. I. Vasilevskiy, Superlattices Microstruct. **22**, 427 (1997).
[58] J. Weberszpil, S. S. Makler, E. V. Anda, and M. I. Vasilevskiy, Microelectron. Eng. **43-44**, 471 (1998).
[59] F. Sols, Ann. Phys. (Leipzig) **214**, 386 (1992).